

Light-off behaviour of PdO/ γ -Al₂O₃ catalysts for stoichiometric CO–O₂ and CO–O₂–NO reactions: a combined catalytic activity–in situ DRIFTS study

A. Martínez-Arias,^{a,*} A.B. Hungría,^a M. Fernández-García,^a A. Iglesias-Juez,^a
J.A. Anderson,^b and J.C. Conesa^a

^a Instituto de Catálisis y Petroleoquímica, CSIC, Campus Cantoblanco, 28049 Madrid, Spain

^b Division of Physical and Inorganic Chemistry, University of Dundee, Dundee DD14HN, Scotland, United Kingdom

Received 28 April 2003; revised 12 June 2003; accepted 13 June 2003

Abstract

Three PdO/ γ -Al₂O₃ catalysts differing in Pd loading (between 0.05 and 1 Pd wt%) have been examined with regard to their light-off catalytic activity for CO oxidation and NO reduction reactions under stoichiometric conditions. Catalytic activity results are explained on the basis of DRIFTS analysis of the adsorbed species present under reaction conditions. It is shown that differences between the catalysts (apart from the expected increasing activity with the Pd loading for both reactions) are considerably greater for NO reduction than for CO oxidation reactions. This is explained by structural differences between the active metallic Pd particles formed during the particle nucleation/growth process that takes place during the course of the light-off run upon interaction with the reactant mixture. On the basis of differences in the natures and relative intensities of adsorbed CO and NO species present during competition for atop and bridging sites over the Pd particles, the correlation (within the Pd loading studied) between NO reduction capability and Pd loading is attributed to the increasing NO dissociation efficiency as the relative size of the particles formed during the course of the reaction is increased.

© 2003 Elsevier Inc. All rights reserved.

Keywords: Pd/ γ -Al₂O₃ catalysts; CO oxidation; NO reduction; Light-off catalytic activity; In situ DRIFTS

1. Introduction

Three-way catalysts (TWC) have been widely used to reduce pollutant emissions from gasoline engine-powered vehicles [1]. Basic components of these systems usually include Rh, Pt, and/or Pd as active metals, zirconia-ceria as promoter, and alumina as a high surface thermally stable support [1,2]. More recently, considerable attention has been paid to the use of Pd as the single active metal component in TWC on the basis of economical aspects (the high cost and limited supply of Rh) and the availability of cleaner fuels and considering also its remarkable activity for oxidation reactions [3,4]. However, some limitations are apparent for Pd-only TWC with respect to their performance in NO reduction reactions [4–6]. This is partly linked to the controversy existing with respect to the optimum cata-

lyst configuration in terms of which metal–oxide interactions (Pd–alumina, Pd–promoter or both) are most favourable in promoting NO reduction reactions [4,7,8], in particular during the light-off period during which the greatest proportion of the whole toxic emission is produced over a driving cycle [1]. Thus, some reports show that introduction of the Ce-containing promoter to the Pd-only catalyst produces a decrease in NO conversion at relatively low temperatures (around 600 K) although it is enhanced at higher temperatures (around 770 K) [4], suggesting that Pd–promoter interactions may be detrimental for light-off performance of the system. However, other authors propose that oxygen vacancies created upon reduction of the promoter in the proximity of palladium can act as promoting sites for NO reduction, leading to an enhanced NO conversion during light-off [7,8]. It is possible that the reasons behind these discrepancies lie mainly in differences in the particular configuration of active components present in each specific case. Such differences may significantly affect NO reduction

* Corresponding author.

E-mail address: amartinez@icp.csic.es (A. Martínez-Arias).

processes given the structural dependency of NO activation processes over Pd catalysts and the dynamic operating mode of the TWCs, which may induce important redox changes in the active components as a function of the variable atmosphere [1,9]. These aspects have motivated the present study, in which preoxidised Pd/Al₂O₃ catalysts differing in the Pd loading present in each case were examined with the aim of determining the factors affecting their light-off performance for CO oxidation–NO reduction processes under different conditions of Pd dispersion/interaction with the alumina support. For this purpose, the catalytic activity of the systems under stoichiometric CO–O₂ and CO–O₂–NO light-off conditions has been examined in combination with in situ DRIFTS results in order to correlate catalytic properties with the state of the catalyst surface and the processes taking place on it under reaction conditions.

2. Experimental methods

Three Pd/Al₂O₃ catalysts (with 0.05, 0.5, and 1 wt% metal loadings) were prepared by incipient wetness impregnation of a γ -Al₂O₃ support (supplied by Condea, $S_{\text{BET}} = 180 \text{ m}^2 \text{ g}^{-1}$) with aqueous solutions of Pd(NO₃)₂ · x H₂O, followed by drying overnight at 383 K and calcination under air at 773 K for 2 h.

Catalytic tests using stoichiometric mixtures of 1% CO + 0.5% O₂ or 1% CO + 0.45% O₂ + 0.1% NO (N₂ balance) at $3 \times 10^4 \text{ h}^{-1}$ were performed in a Pyrex glass flow reactor system. Gases were regulated with mass flow controllers and analysed online using a Perkin–Elmer 1725X FTIR spectrometer coupled with a multiple reflection transmission cell (Infrared Analysis, Inc.). Oxygen concentrations were determined using a paramagnetic analyser (Servomex 540A). The experimental error in conversion values obtained under these conditions was estimated as $\pm 7\%$. Prior to catalytic testing, in situ calcination under synthetic air at 773 K was performed, followed by cooling in synthetic air and a N₂ purge at room temperature. A characteristic test consisted of increasing the temperature from 298 to 823 K at 5 K min^{-1} . Catalyst particles in the 0.125–0.250 mm range were selected after pelleting, grinding and sieving in order to minimise the pressure drop and internal diffusion effects during the catalytic tests. The absence of significant external diffusion effects was also evidenced by the similar activity profiles obtained during tests at $30,000 \text{ h}^{-1}$ under different flow conditions.

DRIFTS analysis of adsorbed species on the catalyst under reaction conditions was carried out using a Perkin–Elmer 1750 FTIR spectrometer fitted with an MCT detector. The DRIFTS cell (Harrick) was fitted with CaF₂ windows and a heating cartridge that allowed samples to be heated to 773 K. Samples of ca. 80 mg were calcined in situ (in a way similar to what was employed for the catalytic tests) and then cooled to 298 K in synthetic air before the reaction mixture was introduced and heated at 5 K min^{-1} up to 673 K,

recording one spectrum (average of 25 scans at 4 cm^{-1} resolution) generally every 15–20 K. The gas mixture (using the same concentrations as employed for the catalytic tests) was prepared using a computer-controlled gas blender with ca. $75 \text{ cm}^3 \text{ min}^{-1}$ passing through the catalyst bed at atmospheric pressure, which roughly corresponds to the space velocity condition employed for the reaction tests. Online NO_x analysis at the outlet of the IR chamber was performed by chemiluminescence (Thermo Environmental Instruments 42C).

3. Results and discussion

The main results of the light-off catalytic activity tests for the CO–O₂ and CO–O₂–NO reactions are shown in Fig. 1. Results obtained for the CO oxidation with oxygen alone show a gradual shift of CO conversion values to higher temperature with decreasing Pd loading. The form of the curves shows a kind of “staircase” shape for the 1% Pd catalyst and, to a lesser extent, for the 0.5% Pd one; this may also occur for the 0.05% Pd catalyst although it shows a smoother profile in this respect. Different factors could account for these irregularities, such as the presence of deactivation phenomena resulting from self-poisoning effects or catalytic interferences among reactants or intermediates [5,9,10]. Another possibility, considering the essentially transient character of these experiments, is related to the occurrence of changes in the number or nature of active sites during the course of the reaction as a consequence of the interactions of the catalyst with the reactant atmosphere. This point will be addressed later when examining in situ DRIFTS results.

The presence of NO in the reactant mixture produced a shift to higher temperature for the light-off of CO with O₂. The magnitude of this shift is generally larger for the 1% Pd catalyst than for the other two catalysts, the inhibiting effect of NO on CO oxidation being particularly strong for the 1% Pd catalyst at the lower conversion temperatures ($\Delta T_{20} = 82, 23, \text{ and } 46 \text{ K}$, while $\Delta T_{50} = 34, 22, \text{ and } 25 \text{ K}$, for the 1, 0.5, and 0.05% Pd catalysts, respectively; T_x refers to the $x\%$ isoconversion temperature). Important differences between the catalysts were observed comparing the ability of the two oxidants (O₂ and NO) for oxidizing CO in each case. Analysis of the CO and NO conversion values during runs under CO–O₂–NO shows that while CO oxidation with NO is strongly favoured with respect to the CO oxidation with O₂ for the 1% Pd catalyst, the opposite occurs for 0.05% Pd while the 0.5% Pd catalyst represents an intermediate case in which CO oxidation with both NO and O₂ takes place almost simultaneously. As a consequence, the range of activities amongst the catalysts are much greater for NO reduction than for CO oxidation with O₂. In fact, analysis of the N₂O yield profile indicates that the 1% Pd catalyst is active for NO reduction even from 303 K, in contrast with the other two catalysts. For this analysis, it must be noted that the first two to four NO conversion points

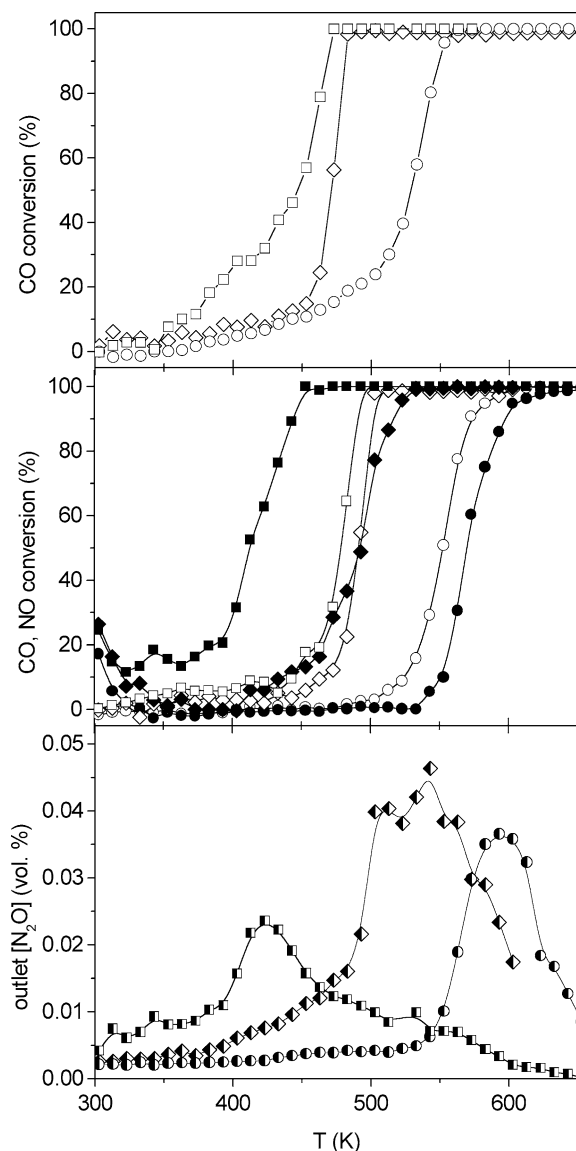


Fig. 1. Main results obtained during light-off tests under stoichiometric CO-O_2 (top) and $\text{CO-O}_2\text{-NO}$ (middle and bottom) for the 1% $\text{Pd/Al}_2\text{O}_3$ (squares), 0.5% $\text{Pd/Al}_2\text{O}_3$ (rhombi), and 0.05% $\text{Pd/Al}_2\text{O}_3$ (circles) catalysts. In the middle, full and open symbols correspond to NO and CO conversion, respectively.

(below ca. 330 K) present a certain contribution corresponding to NO adsorption processes and not to NO reduction processes, as inferred from mass balance analysis. Concerning N_2O selectivity during the NO reduction process, analysis of the N_2O yield shows that N_2O formation increases up to a maximum (lower for the 1% Pd catalyst), roughly following the initial NO conversion profiles, and then decreases, the catalysts becoming almost fully selective to N_2 at high temperatures. This indicates that the N_2O selectivity gradually decreases with the reaction temperature with the catalysts showing almost full N_2O selectivity for the reduction process during the first low-temperature NO reduction stage.

Different factors can be considered as playing a role in the different CO oxidation and NO reduction behaviours ob-

served for the catalysts. Pd can be assumed to be present initially as an oxidised phase in all the catalysts, as a result of the oxidising preconditioning that has been applied to the samples. This has been verified for samples similar to those studied here by in situ XANES studies, which showed the evolution from an inactive PdO -type state to the active metallic Pd state during the course of an experiment performed under stoichiometric $\text{CO-O}_2\text{-NO}$ under conditions similar to those employed here [11]. In this respect, for comparative purposes, it must be taken into account that the Pd reduction process taking place during the course of the reaction may depend to some extent on the degree of interaction between the oxidised Pd species and the alumina support, i.e., a greater degree of difficulty for reduction of oxidised Pd is expected as the degree of interaction with alumina (which, in principle, can be enhanced by decreasing the size of the oxidised Pd entities) is increased [12]. On the other hand, it is necessary to consider the important sensitivity of NO activation/reduction processes on the structural details of the metallic Pd particles present under reaction conditions, in terms of not only particle size but also particle shape [9,13]. Another aspect to consider is the temperature and structure dependences of adsorption/activation competition processes between the different reactants [9,14–17]. In order to clarify these aspects, two of the samples (the 0.5 and 1% Pd samples) have been examined by in situ DRIFTS (Figs. 2–6). Unfortunately, in the 0.05% Pd sample the low Pd loading did not permit a reliable analysis by this technique since the very weak signals obtained for the species chemisorbed on Pd were masked by a much more intense CO(g) signal.

Certain differences were noted comparing $\text{CO}_2\text{(g)}$ and NO(g) evolutions between experiments in Figs. 1 and 3. These must be mainly attributed to differences in the geometry and/or reactant flow conditions of the catalytic reactors between both types of experiment. Nevertheless, qualitative correlation between experiments was apparent. The results obtained during the CO-O_2 reaction over both catalysts show the formation of basically two types of carbonyl species (Figs. 2A and 2B). In the first place is a band at $2099\text{--}2066\text{ cm}^{-1}$, which shifts to lower wavenumber and shows a decrease in intensity with increasing reaction temperature; this corresponds to atop carbonyl species chemisorbed on metallic palladium particles [8,12,14–18]. Second, a band appears at $1980\text{--}1968\text{ cm}^{-1}$, which grows appreciably with reaction temperature (but slightly decreases at 463 K with concomitant downward shift for the 1% Pd sample) and whose frequency shows a maximum at intermediate reaction temperatures. This can be attributed to carbonyl species chemisorbed on bridging sites of metallic palladium particles [8,11,14–18]. Roughly in parallel with the latter, a third carbonyl species appears as a low-frequency shoulder extending to $1850\text{--}1800\text{ cm}^{-1}$. Its position is not well defined due to its relatively large linewidth and its overlap with the $1980\text{--}1968\text{ cm}^{-1}$ bridged carbonyl band. This shoulder can be attributed to carbonyl species chemisorbed on threefold hollow sites of the metallic pal-

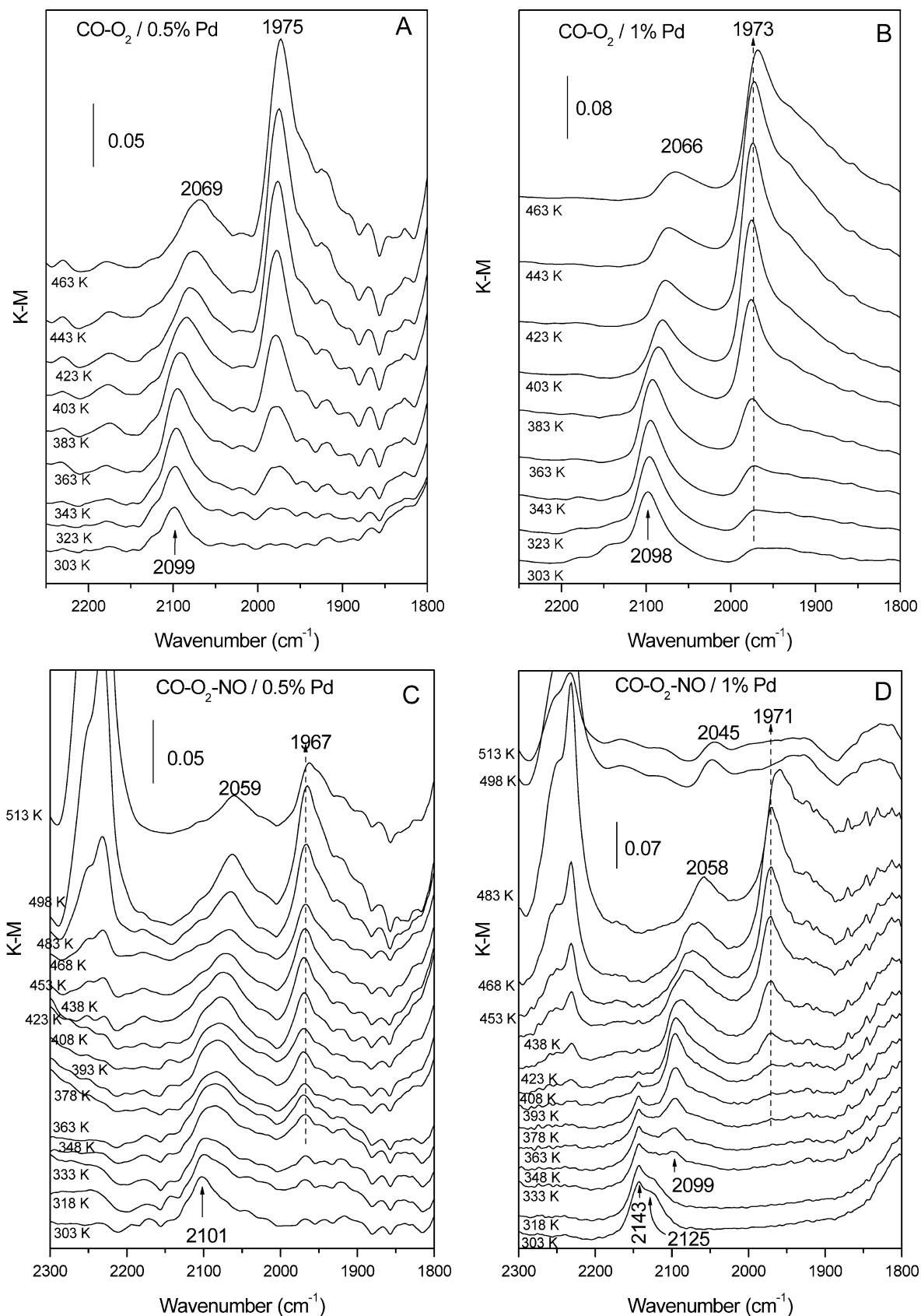


Fig. 2. DRIFTS spectra taken at the indicated temperatures under stoichiometric CO-O₂ (A, B) and CO-O₂-NO (C, D) for the 0.5% Pd/Al₂O₃ (A, C) and 1% Pd/Al₂O₃ (B, D) samples. A reference spectrum containing exclusively the CO(g) bands has been employed to subtract the corresponding contribution from each spectrum in order to isolate contributions from chemisorbed species.

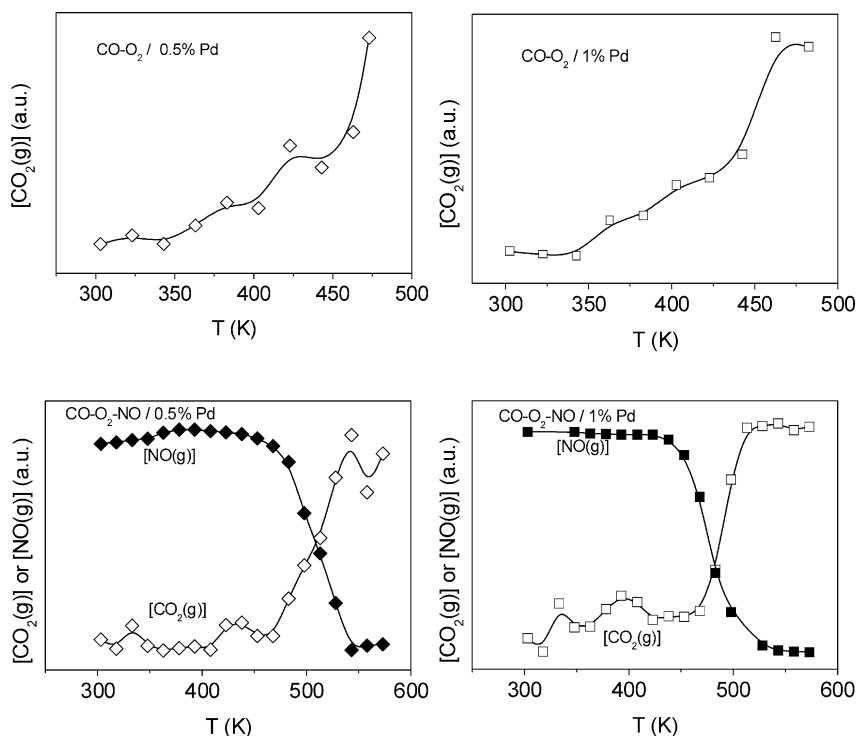


Fig. 3. Results of online analysis of DRIFTS experiments showing the evolution of integrated contribution of $\text{CO}_2(\text{g})$ bands observed by DRIFTS and the NO_x signal of the chemiluminescence detector obtained over the course of the indicated experiments.

ladium particles [18,19]. Both catalysts show an increase in bridged/atop carbonyl intensity ratio with the reaction temperature. This evolution can be attributed, in accordance with previous studies [20,21], to the fact that the relative size of the metallic palladium particles increases with the reaction temperature during the course of the $\text{PdO} \rightarrow \text{Pd}$ reduction process that occurs (in agreement with the general increasing intensity of metallic palladium carbonyls and as confirmed by in situ XANES experiments performed over catalysts similar to the ones studied here, as found elsewhere [11]) upon interaction with the reactant mixture. This hypothesis obviously assumes that low-temperature O_2 adsorption, which most likely would preferentially involve covering of bridging sites [22], must be strongly inhibited under the CO-rich conditions employed [23]. The main difference between both catalysts in the process of genesis of the metallic Pd particles concerns a somewhat greater difficulty in generation of bridging sites in the 0.5% Pd sample (compare Figs. 2A and 2B). This can be related to the lower metallic Pd particle size achieved for the sample with lower Pd loading during the process of nucleation/growth of metallic particles. This becomes more apparent at the lower reaction temperatures for which only incipient germs of the metallic Pd particles have apparently developed.

A fair degree of correlation was observed (Fig. 4) between the frequency decrease of the atop carbonyl band and the CO oxidation rate taking into account that the frequency position of the palladium carbonyls is mainly determined (for each type of carbonyl) by dipolar coupling effects (those corresponding to atop species being the most sensitive

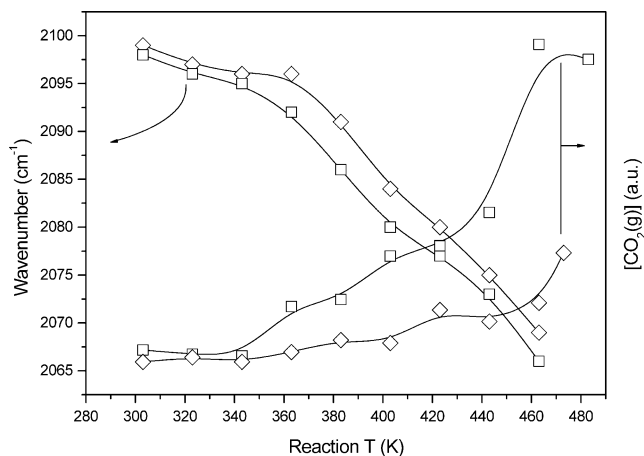


Fig. 4. Wavenumber shift of the atop carbonyl adsorbed on metallic Pd particles and $\text{CO}_2(\text{g})$ evolution as a function of the reaction temperature during the light-off runs under CO-O_2 in the DRIFTS cell for 0.5% $\text{Pd/Al}_2\text{O}_3$ (rhombi) and 1% $\text{Pd/Al}_2\text{O}_3$ (squares).

to coupling [24]), which increases with coverage. The observed evolution indicates, as widely demonstrated [19,25], that the reaction is limited by thermal desorption of CO from the metallic Pd particles within the typical Langmuir–Hinshelwood kinetic scheme. This also agrees with the relatively sharp termination (at values approaching 100% conversion) of the light-off profiles for both catalysts (1 and 0.5%, Fig. 1), which is typical of negative order kinetics for the relevant reactant [26] (CO in this case), as expected when the catalyst operates under the aforementioned limit-

ing step [19]. It somewhat contrasts with the approach to a sigmoidal-type termination of the profile for the 0.05% Pd catalyst (Fig. 1), which suggests [26] that the catalyst may be operating under a different kinetic regime in which the reaction is essentially limited by the rate of CO adsorption on the Pd particles (i.e., it becomes positive order with respect to CO), as expected at the relatively high conversion temperatures at which it is active [19]. Some limitation for Pd reduction may also appear in this sample as a consequence of PdO-support interaction [12], which can also limit to some extent the onset of CO oxidation. On the other hand, the similarities in the shapes of the CO conversion or CO₂ production profiles between the 0.5 and the 1% catalysts (Figs. 1 and 3) suggest that the main differences between them are essentially related to the different numbers of active centres present in each case. In this respect, it must be considered that the nucleation/growth process of formation of active metallic particles is practically the same for both catalysts (according to DRIFTS results in Figs. 2A and 2B) and that the small structural differences between the particles formed for each catalyst (as discussed above) are not reflected in strong kinetic changes for the CO–O₂ reaction, according to the essentially structurally insensitive character of this reaction over Pd [19]. Nevertheless, the increase in the number of active sites occurring as a consequence of the progressive growth of metallic particles during the course of the reaction for any of the catalysts may well be responsible for the irregularities (giving rise to the staircase-type shape mentioned) observed in the activity profiles at lower temperature.

Important differences are observed comparing DRIFTS spectra in the absence and in the presence of a small amount of NO in the reactant mixture (Fig. 2). Such differences are more acute for the 1% Pd sample, which is in agreement with the greater effect of NO on the CO oxidation catalytic properties of this system. Thus, an important suppression on the formation of metallic Pd carbonyls is observed for the latter catalyst, most particularly at lower reaction temperatures (compare Figs. 2B and 2D), while new features at 2143 and ca. 2125 cm⁻¹ (sh) are observed at $T < \sim 423$ K and show decreasing intensity with increasing reaction temperature. These bands can be attributed to atop carbonyl species chemisorbed at oxidised Pd sites [8,19]. Bands due to metallic Pd carbonyl species (atop carbonyls at 2098–2044 cm⁻¹ and bridged carbonyls at 1970–1920 cm⁻¹) begin to appear only at $T \geq 333$ K for this sample (Fig. 2D). Although both bands generally show lower intensity in the presence of NO, it is worth noting that bridged carbonyls are comparatively more affected by this adsorbate. The evolution of the frequency shifts observed for these carbonyls by increasing the reaction temperature correlates well with the catalytic activity for CO oxidation, in a manner similar to that shown above. Additionally, two bands at 2232 and ca. 2250 cm⁻¹, corresponding to NCO species chemisorbed on alumina [8,17], were observed at $T \geq 393$ K and showed maximum intensity in spectra of the sample at 498 K. These

isocyanate species are proposed to be formed following NO dissociation on the metallic palladium particles and subsequent N–CO reaction and spillover onto the alumina support where they accumulate [8,17,27,28]. It can be noted that the onset temperature for their formation correlates well with the increase in the NO reduction catalytic activity, as also noted in previous studies [8,11]. According to a recent report [28], the isocyanate species formed in this kind of catalyst are relatively little reactive toward NO + O₂ mixtures and can thus be considered spectators under the conditions employed here; nevertheless, they can present an interesting practical role as intermediates in the formation of ammonia upon interaction with components of the automobile exhaust gases [28].

As mentioned above, significant differences are observed between the 0.5 and the 1% Pd samples with respect to the formation/evolution of the different Pd carbonyl species in the presence of NO (Figs. 2C and 2D). Thus, the extent to which NO hinders the formation of metallic Pd carbonyls at low reaction temperatures is considerably less for the 0.5% Pd sample. Common to both samples, the presence of NO influences the formation of bridging species to a greater extent than the atop carbonyls. However, for the 0.5% Pd sample, atop species adsorbed on metallic Pd particles are clearly formed even after the initial contact at low temperature with the reactant mixture, while the presence of atop species adsorbed on oxidised Pd entities appears negligible. It is interesting to note that the onset of NO reduction for both samples (at ca. 393 and 423 K for the 1 and 0.5% samples, respectively), in accordance with the initial detection of chemisorbed isocyanate species (Figs. 2C and 2D) and in reasonable agreement with catalytic activity results (Fig. 1) and online gas analysis (Fig. 3), coincides with a sharp increase in the population of bridged carbonyl species.

The increase in NO reduction activity with Pd loading is in line with literature results showing that this activity increases with the relative size of the metallic Pd particles, at least up to a certain limiting value [9,13]. In our particular case, the reasons behind this behaviour can be related, on the basis of DRIFTS results, to the particular CO–NO competition for atop–bridging sites on the active metallic palladium particles and to the NO dissociation capability as a function of the size/structural details of the particles formed during the course of the light-off run. The main difference between the catalysts is related to the presence of oxidised Pd carbonyls (bands at 2143–2125 cm⁻¹) for the 1% Pd sample at low reaction temperatures. The formation of these carbonyls may result from dissociative NO adsorption on the Pd particles, which leads to the formation of the oxidised Pd (Pdⁿ⁺) chemisorption sites. This is consistent with the catalytic activity results (Fig. 1), which show that the 1% Pd sample is able to dissociate NO even at 303 K. Formation of the Pdⁿ⁺ sites can be associated with the presence of NO in the reactant stream on the basis of comparison between DRIFTS experiments conducted in the presence and absence of this oxidant (Fig. 2). These oxidised Pd species can be

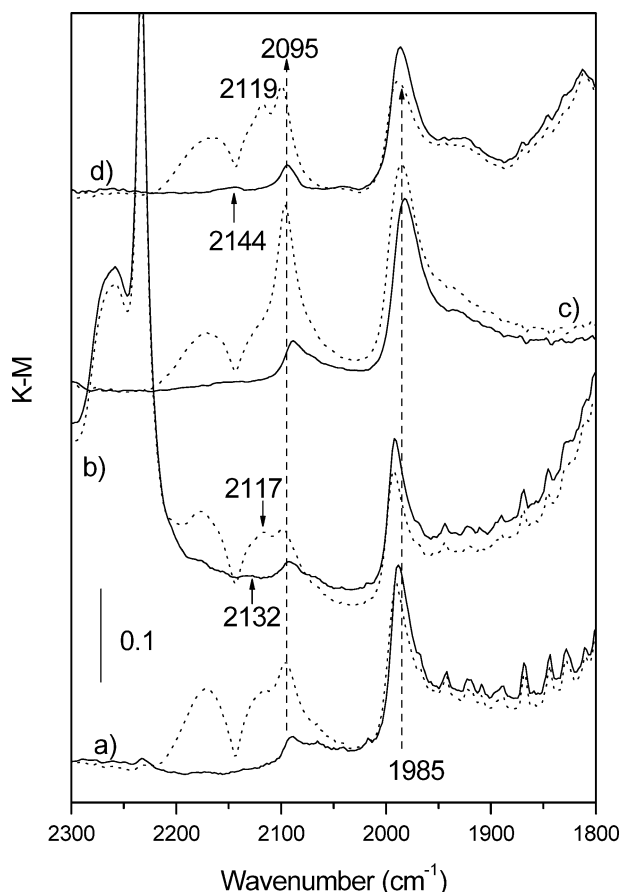


Fig. 5. Postreaction DRIFTS experiments at 303 K for (a, b) 0.5% Pd/Al₂O₃ and (c, d) 1% Pd/Al₂O₃. Following the run under CO–O₂ up to 483 K, the sample was cooled under N₂ and then 1% CO was flowed through the cell (a, c) (dotted line) and subsequently flushed with N₂. (b, d) Same as the former, but after the CO–O₂–NO reaction up to 573 K.

formed during the whole run, even if only in small amounts, as demonstrated by postreaction experiments (Fig. 5). These data again support the proposal that oxidised Pd sites are linked with the presence of NO in the reactant stream. The stabilization of these Pdⁿ⁺-bonded carbonyls in significant quantities only at lower reaction temperatures can be related to their lower thermal stability with respect to carbonyl species adsorbed on metallic particles, as evidenced by the respective behaviour toward flushing with N₂ at room temperature (Fig. 5). The combined results suggest a greater NO dissociation efficiency on the particles formed for the 1% Pd sample. This can be used to explain the greater activity of such a catalyst, taking into account that the NO dissociation process has been proposed as rate limiting, at least for relatively low temperatures and within a range of relatively small particle sizes [13,29].

By considering the influence of NO on the relative amounts of atop-bridging adsorption sites, indicated by the respective carbonyl intensities, one would expect a relatively stronger interaction of NO with bridging sites and with the 1% Pd catalyst. The analysis of the region relevant to adsorbed nitrosyl species is complicated as a consequence of

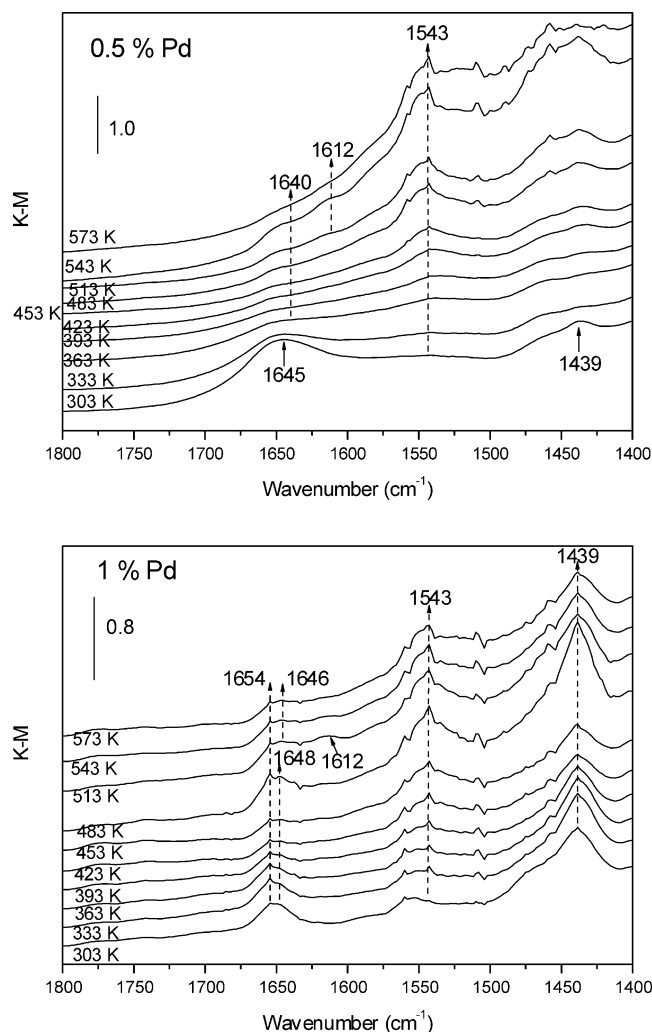


Fig. 6. DRIFTS spectra under CO–O₂–NO at the indicated temperatures in the region relevant to adsorbed nitrosyl species for 0.5% Pd/Al₂O₃ (top) and 1% Pd/Al₂O₃ (bottom).

the relatively low $P_{\text{NO}}/P_{\text{CO}}$ employed for the catalytic experiments as well as the presence of overlapping bands due to species chemisorbed on the support. Thus, the spectra of both samples (Fig. 6) show bands due to bicarbonate species adsorbed on the alumina (at 1654 and 1439 cm⁻¹) [30] and of species giving a band at 1543 cm⁻¹ that grew with the reaction temperature and can be assigned to nitrate species chemisorbed on alumina [30]. A more careful analysis of this region reveals the presence of bands at 1648–1640 (showing a slight high-temperature red shift) and 1612 cm⁻¹ that may be attributed to nitrosyl species chemisorbed on bridging sites of the metallic Pd particles [14–16]. No hint of formation of atop nitrosyl species (expected to give a band at 1750–1730 cm⁻¹ [15–17]) was observed in these spectra, which suggests that when both CO and NO are present under the employed conditions, the latter molecule interacts preferentially with bridging sites while CO forms mainly atop species through either exchange or NO-induced site transfer (bridging → atop [14,17]) processes. Compar-

ison of bridging nitrosyl species for both catalysts reveals that, surprisingly, the 0.5% Pd catalyst appears to sustain a greater amount of such species at low temperature (considering the greater extinction coefficient of the bicarbonate band at 1439 cm^{-1} with respect to that of the overlapping band at 1654 cm^{-1} for this analysis [30]). NO reverse spillover effects, which would be favoured when a higher amount of support (i.e., for lower metal loading) is exposed, may also play a role in this observation [13]. Nevertheless, the observed results are compatible with the higher NO reduction activity of the 1% Pd catalyst and apparently reflect the more efficient NO dissociation over this catalyst within the balance of NO adsorption/dissociation processes taking place on the surface of the catalysts.

4. Conclusions

A combined catalytic activity in situ DRIFTS study of stoichiometric CO–O₂ and CO–O₂–NO reactions over PdO/ γ -Al₂O₃ catalysts with different Pd loadings has been carried out. Results for the CO–O₂ reaction are in line with many studies in the literature showing that the catalysts follow typical Langmuir–Hinshelwood kinetics in which the reaction is initially rate limited by CO desorption from the metallic particles except for a sample with a very small Pd loading for which the reaction onset is shifted to significantly higher temperatures, in which case CO adsorption may become the rate-determining step for the reaction. The light-off profiles show certain irregularities at low reaction temperatures which are attributed to the fact that the number of active sites undergoes a change during the course of the reaction as a consequence of the process of formation of metallic Pd particles. A comparison between the catalyst activities for CO oxidation and NO reduction under stoichiometric CO–O₂–NO reveals significant differences for NO reduction processes. These are explained on the basis of different structural characteristics of the Pd particles formed in each case following interaction with the reactant mixture. In this respect, it is shown that NO dissociation (which may be the rate-determining step under the employed conditions) is most favoured over the larger Pd particles formed for the highest loaded sample, as deduced from catalytic activity results and DRIFTS analysis of the nature (redox state and coordination number of the adsorption site) and the relative intensities of atop–bridging carbonyl or nitrosyl species formed for each catalyst.

Acknowledgments

A.B.H. and A.I.-J. thank the Comunidad de Madrid for grants under which this work has been carried out and

(A.B.H.) for financial help under the “Ayudas para estancias breves en centros de investigación extranjeros” program. Thanks are due to Dr. R. Cataluña for the preparation of some of the catalysts. Financial help by project CICYT (Ref. MAT 2000-1467) is also acknowledged.

References

- [1] E.S.J. Lox, B.H. Engler, in: G. Ertl, H. Knözinger, J. Weitkamp (Eds.), *Environmental Catalysis*, Wiley–VCH, New York, 1999, p. 1.
- [2] R.M. Heck, R.J. Farrauto, *Appl. Catal. A* 221 (2001) 443.
- [3] A. Martínez-Arias, M. Fernández-García, A.B. Hungria, A. Iglesias-Juez, K. Duncan, R. Smith, J.A. Anderson, J.C. Conesa, J. Soria, *J. Catal.* 204 (2001) 238.
- [4] Z. Hu, C.Z. Wan, Y.K. Lui, J. Dettling, J.J. Steger, *Catal. Today* 30 (1996) 83.
- [5] J.R. González-Velasco, J.A. Botas, R. Ferret, M.P. González-Marcos, J.-L. Marc, M.A. Gutiérrez-Ortiz, *Catal. Today* 59 (2000) 395.
- [6] S. Tagliaferri, R.A. Köppel, A. Baiker, *Appl. Catal. B* 15 (1998) 159.
- [7] J.H. Holles, M.A. Switzer, R.J. Davis, *J. Catal.* 190 (2000) 247.
- [8] A. Martínez-Arias, M. Fernández-García, A. Iglesias-Juez, A.B. Hungria, J.A. Anderson, J.C. Conesa, J. Soria, *Appl. Catal. B* 31 (2001) 51.
- [9] D.R. Rainer, S.M. Vesecky, M. Koranne, W.S. Oh, D.W. Goodman, *J. Catal.* 167 (1997) 234.
- [10] N. Matthes, D. Schweich, B. Martin, F. Castagna, *Top. Catal.* 16/17 (2001) 119.
- [11] M. Fernández-García, A. Martínez-Arias, A. Iglesias-Juez, A.B. Hungria, J.A. Anderson, J.C. Conesa, J. Soria, *J. Catal.* 214 (2003) 220.
- [12] K. Otto, L.P. Haack, J.E. deVries, *Appl. Catal. B* 1 (1992) 1.
- [13] L. Piccolo, C.R. Henry, *J. Mol. Catal. A* 167 (2001) 181.
- [14] R. Raval, G. Blyholder, S. Haq, D.A. King, *J. Phys. Condens. Matter* 1 (1989) SB165.
- [15] X. Xu, P. Chen, D.W. Goodman, *J. Phys. Chem.* 98 (1994) 9242.
- [16] S.M. Vesecky, P. Chen, X. Xu, D.W. Goodman, *J. Vac. Sci. Technol. A* 13 (1995) 1539.
- [17] K. Almusaiter, S.C. Chuang, *J. Catal.* 184 (1999) 189.
- [18] I.V. Yudanov, R. Sahnoun, K.M. Neyman, N. Rösch, J. Hoffmann, S. Schauerer, V. Johánek, H. Unterhalt, G. Rupprechter, J. Libuda, H.-J. Freund, *J. Phys. Chem. B* 107 (2003) 255, and references therein.
- [19] X. Xu, D.W. Goodman, *J. Phys. Chem.* 97 (1993) 7711.
- [20] K. Wolter, O. Seiferth, H. Kühlenbeck, M. Bäumer, H.-J. Freund, *Surf. Sci.* 399 (1998) 190.
- [21] M. Frank, M. Bäumer, *Phys. Chem. Chem. Phys.* 2 (2000) 3723.
- [22] T. Engel, G. Ertl, *Adv. Catal.* 28 (1979) 2.
- [23] I. Meusel, J. Hoffmann, J. Hartmann, J. Libuda, H.-J. Freund, *J. Phys. Chem. B* 105 (2001) 3567.
- [24] P. Hollins, *Surf. Sci. Rep.* 16 (1992) 51.
- [25] J. Libuda, I. Meusel, J. Hoffmann, J. Hartmann, L. Piccolo, C.R. Henry, H.-J. Freund, *J. Chem. Phys.* 114 (2001) 4669.
- [26] F. Duprat, *Chem. Eng. Sci.* 57 (2002) 901.
- [27] F. Solymosi, J. Rasko, *J. Catal.* 63 (1980) 217.
- [28] N. Macleod, R.M. Lambert, *Chem. Commun.* (2003) 1300.
- [29] B. Hammer, *J. Catal.* 199 (2001) 171.
- [30] A. Martínez-Arias, M. Fernández-García, A. Iglesias-Juez, J.A. Anderson, J.C. Conesa, J. Soria, *Appl. Catal. B* 28 (2000) 29.